Front. Mater. Sci. 2015, 9(2): 192–198
DOI 10.1007/s11706-015-0294-8

RESEARCH ARTICLE

# Co-substitution of carbonate and fluoride in hydroxyapatite: Effect on substitution type and content

Qing-Xia ZHU (✉), Ya-Ming LI, and Dan HAN

School of Materials Science and Engineering, Jingdezhen Ceramic Institute, Jingdezhen 333001, China



**ABSTRACT: The nanosized hydroxyapatite substituted by fluoride and carbonate ions (CFHA) had been synthesized by aqueous precipitation method. CFHA had been considered as potential bone graft material for orthopedic and dental applications. The objective of this study was to determine the effects of simultaneously incorporated $CO_3^{2-}$ and $F^-$ on the substitution type and content. The morphologies of CFHAs were observed by TEM. The carbonate substitution type and content were characterized by FTIR. The fluoride contents were determined by F-selective electrode. The phase compositions and crystallinity of the samples were investigated by XRD. The fluoride and carbonate contents of CFHA increase with the dopant concentrations nonlinearly. The carbonate substitution has much more obvious effect on morphology compared with the fluoride substitution. The co-existence of $CO_3^{2-}$ and $F^-$ ions can influence the corresponding substitution fraction. The isomorphic substitution of sodium for calcium in the substitution process of $CO_3^{2-}$ can improve crystal degree and favor the B-type substitutions. Due to the closeness of the ion radii and equivalent substitution of $F^-$ and $OH^-$, $F^-$ will occupy the $OH^-$ sites of HA crystals more easily, compelling most of the $CO_3^{2-}$ to be located in the B sites.**

**KEYWORDS: hydroxyapatite; co-substitution; carbonate; fluoride; substitution type; substitution content**

## Contents



Received February 5, 2015; accepted March 15, 2015

E-mail: Qingxia-zhu@163.com

## 1 Introduction

Bone consists of the mineral (hydroxyapatite, HA, $Ca_{10}(PO_4)_6(OH)_2$) and organic (mostly collagen) components [1]. Comprehensive studies have shown that HA is associated with minor elements (e.g. $CO_3^{2-}$, $SiO_4^{4-}$, $Na^+$, $Mg^{2+}$) and trace elements (e.g. $Sr^{2+}$, $K^+$, $Cl^-$ and $F^-$) [2]. However, these doping elements will result in significant changes of HA on the aspects of crystallographic structure,

physic-chemical properties, and *in-vitro* and *in-vivo* performance [3–5].

Carbonate is the chief minor substituent in bone apatite (2.0–8.0 wt.%) [6]. The carbonate group can substitute the hydroxyl ions (A-type) and the phosphate ions (B-type) respectively or substitute two positions at the same time (AB-type) [7]. The ratio of type A to type B in biological apatite is between 0.7 and 0.9 depending on the age of the individual [8]. The presence of B-type carbonate in the apatite lattice was shown to cause a decrease in crystallinity and an increase in solubility both *in vitro* and *in vivo* tests, causing better bioresorbability and osteointegration rate [9], while the human trabecular osteoblastic cells had a lower affinity for the A-CHA surface compared to HA one [10]. The effect of carbonate substitution on structure and performance depends on the substitution content and type.

Fluoride-doped hydroxyapatite is formed by replacing $OH^-$ with $F^-$ over a wide range of concentrations. Fluoride substitution exhibited improved thermal stability and mechanical properties [11–12]. Moreover, $F^-$ ions were shown to promote the mineralization and crystallization of HA in the bone forming process [13]. Furthermore, $F^-$ ions released from synthetic fluoride-doped HA powder can prevent dental caries in a bacteria containing acidic environment [14].

$CO_3^{2-}$ and $F^-$ substitution in apatite have opposite effects on crystallinity and solubility. CFHAs as bone graft materials of desired solubility can be prepared by manipulating the relative contents of $CO_3^{2-}$ and $F^-$ incorporated in the apatite. The aim of the present study was to investigate the effects of the concentrations and adding order of dopant ions, the isomorphic substitution of $Na^+$ ion on the co-substitution type and contents.

## 2 Materials and methods

### 2.1 CFHA preparation

The CFHA powders were prepared by an aqueous precipitation method by dropping the $(NH_4)_2HPO_4$, NaF and $NaHCO_3$ solution into a reactor containing $Ca(NO_3)_2 \cdot 4H_2O$ solution. All the solvents and reagents were analytically grade and were purchased from Shanghai National Chemical Reagent Corporation. The molar ratio $[n(Ca^{2+})/n(PO_4^{3-})]$ was 1.667 which is the stoichiometric $[n(Ca^{2+})/n(PO_4^{3-})]$ ration of HA. The dopant concentrations of sample were listed in Table 1. After mixing, the solution was vigorously stirred for about 3 h and the $pH > 10$ values of the solutions were adjusted by the addition of $NH_4OH$ solution. The reaction temperature of 60°C was maintained by use of a thermostatically controlled hot plate. Finally, after aged for 24 h at room temperature, the precipitate was washed, filtered and dried. In order to prepare Na-free samples, $F^-$ and $CO_3^{2-}$ were introduced using $NH_4F$ and $NH_4HCO_3$ respectively. The difference between samples $1^{\#}$ and $2^{\#}$ with $C_{22}F_8$ is the adding order of fluoride and carbonate sources. First dropping carbonate sources into the pre-stirred mixture of $(NH_4)_2HPO_4$ and $Ca(NO_3)_2 \cdot 4H_2O$ solution, stirring for 4 h, then dropping fluoride sources, designated as sample $1^{\#}$; and vice, firstly dropping fluoride sources, stirring for 4 h, then dropping carbonate sources, designated as sample $2^{\#}$.

### 2.2 Characterization

The morphological features and particle sizes of the

**Table 1** The dopant concentration and the substitution content of samples

| Sample | $n(CO_3^{2-})/n(PO_4^{3-})$ | $n(F^-)/n(Ca^{2+})$ | With/without Na | Fluoride content /wt.% | Carbonate content /wt.% |
|---|---|---|---|---|---|
| $C_3F_4Na$ | 0.03 | 0.04 | with | 0.424 | 3.20 |
| $C_3F_8Na$ | 0.03 | 0.08 | with | 0.679 | 3.19 |
| $C_3F_{12}Na$ | 0.03 | 0.12 | with | 1.373 | 3.14 |
| $C_{11}F_4Na$ | 0.11 | 0.04 | with | 0.392 | 6.19 |
| $C_{11}F_8Na$ | 0.11 | 0.08 | with | 0.628 | 6.16 |
| $C_{11}F_{12}Na$ | 0.11 | 0.12 | with | 1.268 | 6.13 |
| $C_{22}F_4Na$ | 0.22 | 0.04 | with | 0.362 | 8.21 |
| $C_{22}F_8Na$ | 0.22 | 0.08 | with | 0.558 | 8.17 |
| $C_{22}F_{12}Na$ | 0.22 | 0.12 | with | 1.223 | 8.15 |
| $C_{22}F_4$ | 0.22 | 0.04 | without | 0.441 | 7.21 |
| $C_{22}F_8$ | 0.22 | 0.8 | without | 0.679 | 7.18 |
| $C_3F_{12}$ | 0.03 | 0.12 | without | 1.223 | 2.13 |
| HA | 0 | 0 | with | – | – |
| $C_3HA$ | 0.03 | 0 | with | – | 3.23 |

precipitated powders were investigated by transmission electron microscopy (TEM, TECNAI 12). The infrared (IR) spectra were recorded using KBr pellets (about 1 mg sample per 200 mg KBr) with a spectral resolution of 4 $cm^{-1}$ by Fourier transform infrared spectroscopy (FTIR, Nexus, Nicolet, USA) to evaluate the functional groups of the specimens. It was reported that the ratio of the extinction of the IR carbonate band at about 1420 $cm^{-1}$ ($E_{1420}$) to the extinction of the IR phosphate band at about 570 $cm^{-1}$ ($E_{570}$) is linearly related to the carbonate content of apatites [15]. In experimental conditions, the equation utilized for calculating the carbonate content was $w = 17.4E_{1420}/E_{570} + 0.4$, where $w$ is the carbonate content in mass. The fluoride content of samples was determined by F-selective electrode (Orion94-09) choosing guaranteed reagent NaF as a reference calibration. The phases composition and crystallinity of the samples were investigated by X-ray diffraction (XRD) using a diffractometer (PANalytical X′ pert PRO, Netherlands) with Cu Kα radiation.

## 3 Results and discussion

### 3.1 The effect of dopant ions concentration

As can be seen from Fig. 1, $F^-$ doping had less obvious effects on the morphologies of apatites, which was in accordance with conclusion from Chen et al. [16]. However, crystal size and aspect ratio obviously decreased with the increase of carbonate ions concentration. Since ionic strengths may have a certain effect on the thermodynamics constant, the solubility product of apatite ($K_{sp}$) increases with the increase of carbonate contents. While the driving force of CFHA formation decreased as $\ln K_{sp}$ increased [17], according to the crystal growth theory, the crystals with small aspect ratio and size were prone to be formed under the condition of low driving force.

FTIR spectra of the apatite prepared at different dopant concentrations were shown in Fig. 2. All the spectra showed the typical bands of the apatite at about 1090–1044 $cm^{-1}$ ($PO_4^{3-}$ asymmetric stretching vibration), 960 $cm^{-1}$ ($PO_4^{3-}$ symmetric stretching vibration), 570 and 600 $cm^{-1}$ ($PO_4^{3-}$ bending vibration) [18].

Obvious vibration peak of O – H at about 630 $cm^{-1}$ was shown in pure HA. The O – H vibration intensity at about 630 $cm^{-1}$ decreased significantly, the peaks at 1550 $cm^{-1}$ ascribed to A-type $CO_3$ appeared, moreover, the 1460 $cm^{-1}$ band (ascribed to the complex of two peaks: $\upsilon_{3a}$ of A-site $CO_3^{2-}$ and $\upsilon_{3b}$ of B-site $CO_3^{2-}$) appeared stronger than that of 1420 $cm^{-1}$ one (ascribed to $\upsilon_{3a}$ of B-site $CO_3^{2-}$) [19], indicating that the predominantly A-CHA in sample $C_3HA$, in accordance with the reports that A-type mostly existed over the carbonate range of 0–4 wt.% [20]. However, O – H peaks at 630 $cm^{-1}$ disappeared in all sample CFHAs, indicating that the co-substitution of $F^-$ and $CO_3^{2-}$ had almost occupied all of $OH^-$ sites in the structure. In the composite-doping samples $C_3F_4Na$ and $C_3F_{12}Na$ with the same $n(CO_3^{2-})/n(PO_4^{3-})$ at 0.03, the 1460 $cm^{-1}$ band appeared slightly weaker than that of 1420 $cm^{-1}$ one, as shown by curves c and f in Fig. 2, indicating that the substitution priority of $F^-$ for $OH^-$ changed the carbonate substitution type and compelled most of the $CO_3^{2-}$ to be located in the B sites.

The intensities of characteristic bands of $CO_3^{2-}$ at about 1460, 1420 and 875 $cm^{-1}$ increased with increasing $n(CO_3^{2-})/n(PO_4^{3-})$, as shown by curves d and e in Fig. 2, indicating that structural carbonate contents increased with the carbonate concentrations. However, the actual substitution contents still had a quite deviation from the theoretical calculation (assuming the substitution mechanism as follows: $F^-$ substituted $OH^-$, $CO_3^{2-}$ only substituted $PO_4^{3-}$, and moreover, the part of $Ca^{2+}$ were substituted by

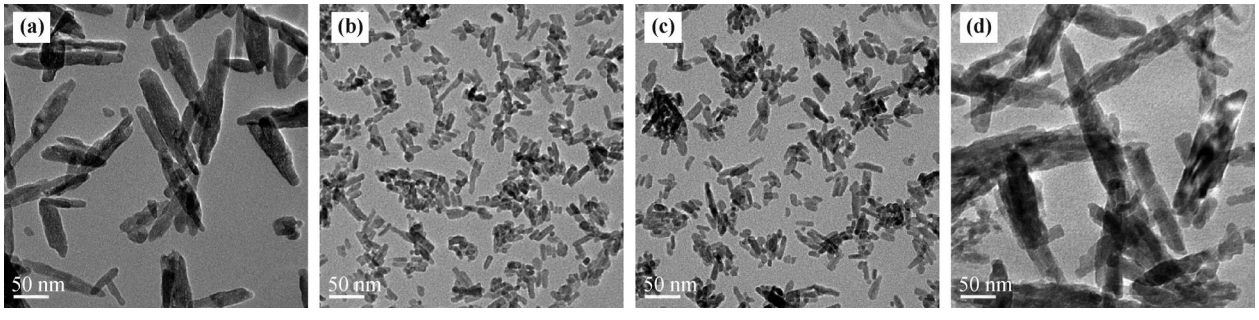


**Fig. 1** TEM photographs of CFHAs prepared at different dopant concentrations: **(a)** $C_3F_4Na$; **(b)** $C_{22}F_{12}Na$; **(c)** $C_{22}F_4Na$; **(d)** $C_3F_{12}Na$.

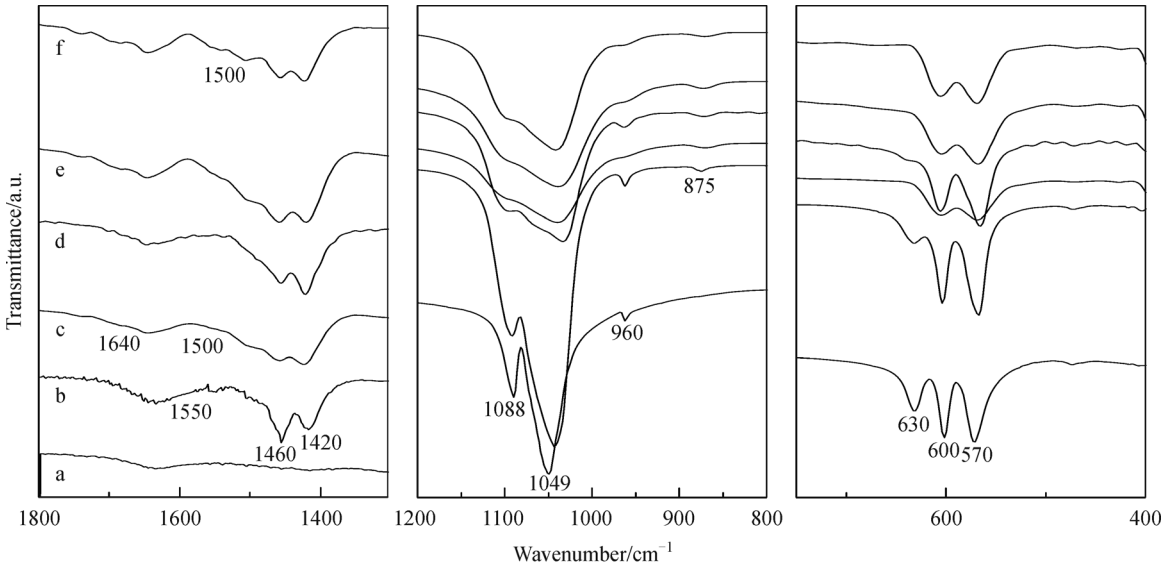


**Fig. 2** FTIR spectra of the apatites prepared at different dopant concentrations: HA (a); $C_3HA$ (b); $C_3F_4Na$ (c); $C_{22}F_{12}Na$ (d); $C_{22}F_4Na$ (e); $C_3F_{12}Na$ (f).

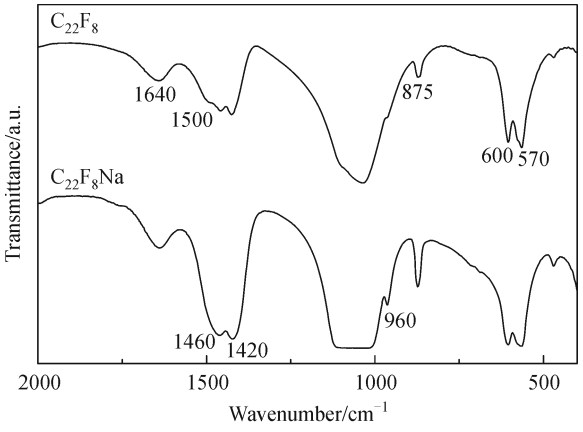


**Fig. 3** FTIR spectra of CFHAs using $NH_4HCO_3$ or $NaHCO_3$ as reactants introducing $CO_3$ groups.

$Na^+$ in order to compensate the electricity imbalance). For example, according to the dopant molar ratios, the theoretical carbonate and fluoride contents of sample $C_{22}F_{12}Na$ should be 6.82 and 2.14 wt.%, respectively, compared with the test data of 8.15 and 1.223 wt.%, as shown in Table 1. Due to the difference of preparation conditions, on the coexistence condition of $F^-$, $OH^-$, $CO_3^{2-}$, $PO_4^{3-}$, $Ca^{2+}$ and $Na^+/NH_4^+$ ions in the reaction system, there are many possible co-substitution mechanisms which are different from the supposed substitution model [21]. In addition, the higher $CO_3^{2-}$ substitution content can be related to the part of $CO_3^{2-}$ in the A site and surface absorbance of $CO_2$. However, the complexity of $F^-$ substitution process resulted in the actual $F^-$ substitution contents much lower than the theoretical value based on the theory proposed by Tanaka et al. [22]. And it also can be seen from Table 1 that the $F^-$ and $CO_3^{2-}$ substitution contents of CFHA increase with the dopant concentrations nonlinearly. Moreover, on the premise condition of the same dopant concentrations, due to the interference between $F^-$ and $CO_3^{2-}$ co-substitution, the more the carbonate content, the less the fluoride content and vice versa.

### 3.2 The effect of $Na^+$ ions existence

FTIR spectra of both samples (see Fig. 3) clearly show the typical bands of $CO_3^{2-}$-containing apatites. The peak at 1640 cm$^{-1}$ is attributable to the presence of adsorbed water. The intensity of characteristic bands of $CO_3^{2-}$ at about 1460, 1420 and 875 cm$^{-1}$ in sample $C_{22}F_8Na$ are obviously stronger than that in sample $C_{22}F_8$, indicating less content of carbonate in sample $C_{22}F_8$. Due to the low stability of $NH_4HCO_3$ as the $CO_3^{2-}$ source, $NH_4HCO_3$ can be easily eliminated by heating, the concentration of carbonate ions in the solution greatly reduced, and then decreased the carbonate substitute content, as confirmed by the calculation data in Table 1.

Through the computer fitting peak technology, $CO_3^{2-}$

vibration peak in 875 $cm^{-1}$ can be split into two peaks in 873 and 880 $cm^{-1}$ distributed as the Lorentz function. Landi et al. [10] reported that a weight ratio of A- and B-type $CO_3^{2-}$ could be estimated from the intensity ratio of two peaks at 880 and 873 $cm^{-1}$ in the IR spectrum. The analysis showed that A/B-type weight ratios were 0.53 ($C_{22}F_8$) and 0.28 ($C_{22}F_8Na$). Moreover the appearance of the shoulder peak is near 1500 $cm^{-1}$ in sample $C_{22}F_8$, which is attributed to carbonate ions in type A-sites [23], confirming that the presence of $Na^+$ favored the B-type carbonate substitution. According to the molecular-dynamic model [24], $Na^+$ ion was incorporated into CHA more easily than $NH_4^+$, which can be attributed to the difference in ionic radius between $Na^+$ (1.16 Å) and $NH_4^+$ (1.43 Å), meaning that $Ca^{2+}$ (1.14 Å) ions can be more easily replaced by $Na^+$ ions in order to compensate for extra negative charge caused by the B-type substitution of $CO_3^{2-}$ for $PO_4^{3-}$ ions ($CO_3^{2-} + Na^+ \leftrightarrow PO_4^{3-} + Ca^{2+}$) [25].

Due to the high carbonate substitution and low synthesis temperature, both as-prepared precipitates are low-crystallinity HA, as shown in Fig. 4. However, the sample $C_{22}F_8Na$ has more prominent HA peaks compared with the sample $C_{22}F_8$. $CO_3^{2-}$ for $PO_4^{3-}$ coupled $Na^+$ for $Ca^{2+}$ is conductive to keep charge balance. Moreover, the closeness of ion radii of $Na^+$ and $Ca^{2+}$ causes little change of lattice parameters by compensating mismatch of [$CO_3$] and [$PO_4$] group size. Consequently, the introduction of $Na^+$ can reduce the lattice distortion of the carbonate-doped apatites so as to improve its crystallinity.

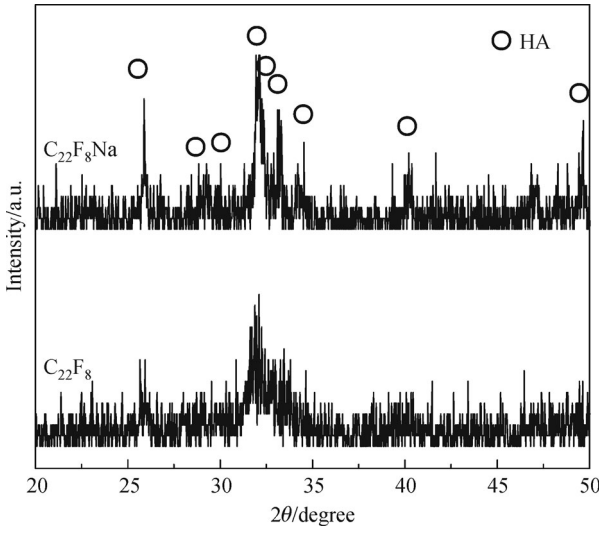


**Fig. 4** XRD patterns of CFHAs using $NH_4HCO_3$ or $NaHCO_3$ as reactants introducing $CO_3$ groups.

### 3.3 The effect of adding order of fluoride and carbonate

The more prominent carbonate vibration peaks indicated the higher carbonation degree of sample 1#, as shown in Fig. 5. When the carbonate sources are introduced into the F-free HA precipitation, carbonate have priority to occupy the [OH] and [$PO_4$] sites, resulting in the higher carbonation degree. However, when the carbonate sources drop into the fluoride-doped apatite precipitation (sample 2#), the possibility of a competition between the pre-existed $F^-$ and the newly introduced $CO_3^{2-}$ for occupation of the OH sites should be considered. Due to the closeness of the ion radii and the equivalent substitution of $F^-$ and $OH^-$, $F^-$ will occupy the $OH^-$ site of HA crystals more easily, compelling most of $CO_3^{2-}$ to be located in the B sites, confirmed by the A/B-type weight ratio analysis of 0.56 (1#) and 0.48 (2#).

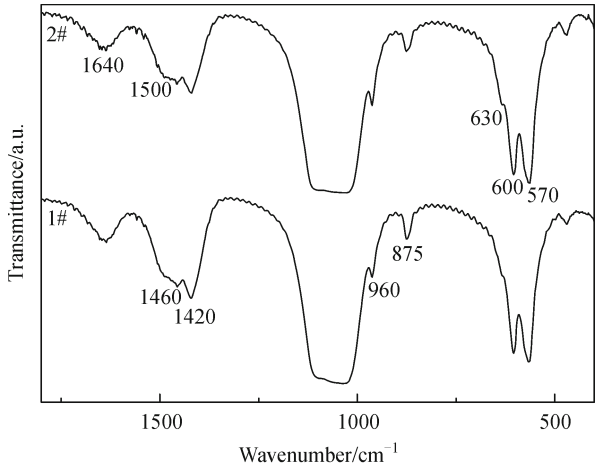


**Fig. 5** FTIR spectra of CFHAs with different adding order of fluoride and carbonate.

## 4 Conclusions

To manipulate the relative contents of $CO_3^{2-}$ and $F^-$ incorporated in the apatite, the effects of the concentrations and adding order of dopant ions, the isomorphic substitution of $Na^+$ ion on the co-substitution type and contents were investigated. The fluoride and carbonate contents of CFHA increase with dopant concentrations nonlinearly. Due to the complexity of substitution mechanism and preparation conditions, the test data and theoretical values of substitution contents have a quite deviation. As a result of the closeness of ion radii of $Na^+$ and $Ca^{2+}$ and charge-balance compensation function, the isomorphic substitu-

tion of $Na^+$ ions can improve crystallinity and favor the B-type carbonate substitutions. The possibility of a competition between $F^-$ and $CO_3^{2-}$ for occupation of the OH sites should be considered in the coexistence condition of dopant ions. Considering the closeness of the ion radii and equivalent substitution of $F^-$ and $OH^-$, $F^-$ will occupy the $OH^-$ site of HA crystals more easily, compelling most of $CO_3^{2-}$ to be located in the B sites.

**Acknowledgements** This work was supported by a grant from the National Natural Science Foundations of China (Grant No. 51462014), funded projects for young scientists of Jiangxi Province (20122BCB23019), "2014 Oceangoing Voyage" project from Jiangxi Science and Technology Association, funded projects from the China Scholarship Council (P-1-00577).

## References

[1] Lafon J P, Champion E, Bernache-Assollant D. Processing of AB-type carbonated hydroxyapatite $Ca_{10-x}(PO_4)_{6-x}(CO_3)_x(OH)_{2-x-2y}(CO_3)_y$ ceramics with controlled composition. Journal of the European Ceramic Society, 2008, 28(1): 139–147

[2] Kay M I, Young R A, Posner A S. Crystal structure of hydroxyapatite. Nature, 1964, 204(4963): 1050–1052

[3] Yao F, LeGeros J P, LeGeros R Z. Simultaneous incorporation of carbonate and fluoride in synthetic apatites: Effect on crystallographic and physico-chemical properties. Acta Biomaterialia, 2009, 5(6): 2169–2177

[4] Zhu Q X, Wu J Q. Effective factors of preparation for carbonated hydroxyapatite by the aqueous precipitation method. Journal of the Chinese Ceramic Society, 2007, 35(6): 690–695

[5] Yao F, LeGeros R Z. Carbonate and fluoride incorporation in synthetic apatites: Comparative effect on physico-chemical properties and *in vitro* bioactivity in fetal bovine serum. Materials Science and Engineering C, 2010, 30(3): 423–430

[6] LeGeros R Z, Trautz O R, Klein E, et al. Two types of carbonate substitution in the apatite structure. Specialia Experientia, 1969, 25(1): 5–7

[7] Ślósarczyk A, Paszkiewicz Z, Paluszkiewicz C. FTIR and XRD evaluation of carbonated hydroxyapatite powders synthesized by wet methods. Journal of Molecular Structure, 2005, 744–747: 657–661

[8] Rey C, Renugopalakrishman V, Collins B, et al. Fourier transform infrared spectroscopic study of the carbonate ions in bone mineral during aging. Calcified Tissue International, 1991, 49(4): 251–258

[9] Morales-Nieto V, Navarro C H, Moreno K J, et al. Poly(methyl methacrylate)/carbonated hydroxyapatite composite applied as coating on ultra-high molecular weight polyethylene. Progress in Organic Coatings, 2013, 76(1): 204–208

[10] Landi E, Tampieri A, Celotti G, et al. Influence of synthesis and sintering parameters on the characteristics of carbonate apatite. Biomaterials, 2004, 25(10): 1763–1770

[11] Zeng L, Zhou H M, Yi D Q, et al. Thermophysical properties and bioactivity research of FHA. Functional Materials, 2010, 41(1): 100–104

[12] Gross K A, Rodríguez-Lorenzo L M. Sintered hydroxyfluorapatites. Part II: mechanical properties of solid solutions determined by microindentation. Biomaterials, 2004, 25(7–8): 1385–1394

[13] Grzanna M, LeGeros R Z, Polotsky A, et al. Fluoride-substituted apatites support proliferation and expression of human osteoblast phenotype *in vitro*. Key Engineering Materials, 2003, 240–242: 695–698

[14] Sakae T, Hoshino K, Fujimori Y, et al. *In vitro* interaction of bone marrow cells with carbonate and fluoride containing apatites. Key Engineering Materials, 2001, 192–195: 347–350

[15] Vagenas N V, Gatsouli A, Kontoyannis C G. Quantitative analysis of synthetic calcium carbonate polymorphs using FT-IR spectroscopy. Talanta, 2003, 59(4): 831–836

[16] Chen Y, Miao X. Effect of fluorine addition on the corrosion resistance of hydroxyapatite ceramics. Ceramics International, 2004, 30(7): 1961–1965

[17] Baig A A, Fox J L, Hsu J, et al. Effect of carbonate content and crystallinity on the metastable equilibrium solubility behavior of carbonated apatites. Journal of Colloid and Interface Science, 1996, 179(2): 608–617

[18] Weng S F. Fourier Transform Infrared Spectrometer. Beijing: Chemical Industry Press, 2005 (in Chinese)

[19] Zhu Q X. Investigation on the preparation, structure and performance of carbonated hydroxyapatite powder and coating. Dissertation for the Doctoral Degree. Guangzhou: South China University of Technology, 2007 (in Chinese)

[20] Kovaleva E S, Shabanov M P, Putlayev V I, et al. Carbonated hydroxyapatite nanopowders for preparation of bioresorbable materials. Materialwissenschaft und Werkstofftechnik, 2008, 39 (11): 822–829

[21] Lee Y, Hahm Y M, Matsuya S, et al. Characterization of macroporous carbonate-substituted hydroxyapatite bodies prepared in different phosphate solutions. Journal of Materials Science, 2007, 42(18): 7843–7849

[22] Tanaka H, Yasukawa A, Kandori K, et al. Surface structure and properties of fluoridated calcium hydroxyapatite. Colloids and Surfaces A, 2002, 204(1–3): 251–259

[23] Rey C, Collins B, Goehl T, et al. The carbonate environment in bone mineral: a resolution-enhanced Fourier transform infrared spectroscopy study. Calcified Tissue International, 1989, 45(3): 157–164

[24] Peroos S, Du Z, de Leeuw N H. A computer modelling study of

the uptake, structure and distribution of carbonate defects in hydroxy-apatite. Biomaterials, 2006, 27(9): 2150–2161

[25] Barinov S M, Fadeeva I V, Ferro D, et al. Stabilization of carbonate hydroxyapatite by isomorphic substitutions of sodium for calcium. Russian Journal of Inorganic Chemistry, 2008, 53(2): 164–168